



Published in final edited form as:

*Ann Vasc Surg.* 2025 January ; 110(Pt A): 522–533. doi:10.1016/j.avsg.2024.08.004.

## Allogenic Vertebral Body Adherent Mesenchymal Stromal Cells Promote Muscle Recovery in Diabetic Mouse Model of Limb Ischemia

Mackenzie K. Madison<sup>1</sup>, Theresa S. Doiron<sup>1</sup>, Jennifer Stashevsky<sup>1</sup>, Nancy Zhang<sup>1</sup>, Marlee Yancey<sup>1</sup>, Chang-Hyun Gil<sup>1</sup>, Hanaa Dakour Aridi<sup>1</sup>, Erik J. Woods<sup>2</sup>, Michael P. Murphy<sup>1</sup>, Steven J. Miller<sup>1</sup>

<sup>1</sup>Department of Surgery, Indiana University School of Medicine, Indianapolis, IN, USA.

<sup>2</sup>Ossium Health Inc., Indianapolis, IN, USA.

### Abstract

**Background:** Chronic limb-threatening ischemia (CLTI) carries a significant risk for amputation, especially in diabetic patients with poor options for revascularization. Phase I trials have demonstrated efficacy of allogeneic mesenchymal stromal cells (MSC) in treating diabetic CLTI. Vertebral bone-adherent mesenchymal stromal cells (vBA-MSC) are derived from vertebral bodies of deceased organ donors, which offer the distinct advantage of providing a 1,000x greater yield compared to that of living donor bone aspiration. This study describes the effects of intramuscular injection of allogenic vBA-MSC in promoting limb perfusion and muscle recovery in a diabetic CLTI mouse model.

**Methods:** A CLTI mouse model was created through unilateral ligation of the femoral artery in male polygenic diabetic TALLYHO mice. The treated mice were injected with vBA-MSC into the gracilis muscle of the ischemic limb 7 days post ligation. Gastrocnemius or tibialis muscle was assessed postmortem for fibrosis by collagen staining, capillary density via immunohistochemistry, and mRNA by quantitative real-time polymerase chain reaction (PCR). Laser Doppler perfusion imaging and plantar flexion muscle testing (MT) were performed to quantify changes in limb perfusion and muscle function.

This is an open access article under the CC BY-NC-ND license (<http://creativecommons.org/licenses/by-nc-nd/4.0/>).

Correspondence to: Mackenzie K. Madison, MD, Division of Vascular Surgery, Department of Surgery, Indiana University School of Medicine, Joseph E. Walther Hall (R3), 980 W. Walnut St., C120, Indianapolis, IN, 46202; madisonm@iupui.edu.  
Dr. Miller is the senior author on this work.

Dr. Steven Miller and Dr. Michael Murphy are Co-Principal investigator of this lab.

Declarations of Interest: None.

#### CREDIT AUTHORSHIP CONTRIBUTION STATEMENT

**Mackenzie K. Madison:** Writing – review & editing, Writing – original draft, Methodology, Investigation, Conceptualization. **Theresa S. Doiron:** Writing – review & editing, Writing – original draft, Methodology, Investigation, Conceptualization. **Jennifer Stashevsky:** Visualization, Investigation. **Nancy Zhang:** Investigation. **Marlee Yancey:** Visualization, Investigation. **Chang-Hyun Gil:** Visualization, Methodology, Investigation. **Hanaa Dakour Aridi:** Writing – review & editing, Investigation. **Erik J. Woods:** Writing – review & editing, Conceptualization. **Michael P. Murphy:** Writing – review & editing, Supervision, Funding acquisition, Conceptualization. **Steven J. Miller:** Writing – review & editing, Writing – original draft, Visualization, Supervision, Project administration, Methodology, Formal analysis.

Meeting Presentation: This work was presented at the 2024 Vascular and Endovascular Surgery Society Annual Meeting in Sun Valley Idaho on January 19th, 2024.

**Results:** Compared to vehicle (Veh) control, treated mice demonstrated indicators of muscle recovery, including decreased fibrosis, increased perfusion, muscle torque, and angiogenesis. PCR analysis of muscle obtained 7 and 30 days post vBA-MSc injection showed an upregulation in the expression of MyoD1 ( $P = 0.03$ ) and MyH3 ( $P = 0.008$ ) mRNA, representing muscle regeneration, vascular endothelial growth factor A (VEGF-A) ( $P = 0.002$ ;  $P = 0.004$ ) signifying angiogenesis as well as interleukin (IL-10) ( $P < 0.001$ ), T regulatory cell marker Foxp3 ( $P = 0.04$ ), and M2-biased macrophage marker Mrc1 (CD206) ( $P = 0.02$ ).

**Conclusions:** These findings indicate human allogeneic vBA-MSc ameliorate ischemic muscle damage and rescue muscle function. These results in a murine model will enable further studies to develop potential therapies for diabetic CLTI patients.

## INTRODUCTION

Chronic limb-threatening ischemia (CLTI) represents the end stage of peripheral arterial disease (PAD) and is characterized by rest pain and/or tissue loss. Over 150,000 lower extremity amputations are performed each year in the United States as a result of CLTI,<sup>1</sup> and diabetic patients present a significantly greater risk for amputation due to poor outcomes from surgical and endovascular procedures for limb preservation.<sup>2</sup> No effective nonsurgical or pharmacological treatment is currently available for CLTI patients, including diabetics, which are without options for interventional revascularization.<sup>3,4</sup>

Cellular-based therapy using autologous bone marrow-derived mononuclear cells (BMD-MNC) to treat CLTI has shown promise for reducing amputation rates in some subpopulations of PAD patients.<sup>5-8</sup> However, clinical results from our group<sup>7,9</sup> and results from other groups<sup>10</sup> have shown that diabetic CLTI patients are largely refractory to cell therapy; thus, this subpopulation of patients require an alternative strategy for successful treatment. The use of allogeneic BMD mesenchymal stromal cell (BMD-MSc) preparations from young, healthy donors has been shown to be a possible approach to enable regenerative therapy for CLTI patients.<sup>11</sup> Preliminary, unpublished data from our clinical trial in patients undergoing amputations for CLTI ([ClinicalTrials.gov](https://clinicaltrials.gov/ct2/show/study/NCT02685098) Identifier: NCT02685098) demonstrate that allogeneic BMD-MSc from young, healthy female donors stimulate angiogenesis to a greater degree than autologous cells in CLTI patients, including diabetics.

A significant issue for treating CLTI with allogeneic BMD-MSc is the relatively low yield of cells from single donors and the resultant need for multiple passages, leading to phenotypic changes and possible replicative senescence.<sup>12,13</sup> The low cell yield per donor also requires the use of multiple donors to generate sufficient cells for clinical purposes, resulting in variable outcomes and potential loss of efficacy.<sup>13</sup> Adherent MSc isolated from vertebral body bone matrix (vertebral bone-adherent mesenchymal stromal cells [vBA-MSc]) provide a potentially superior source of therapeutic cells because of the greatly increased MSc yield per single donor and reduced rate of phenotypic changes after multiple passages.<sup>13</sup> However, their ability to counteract the effects of CLTI, such as decreased perfusion and tissue damage, has not been established, particularly in the context of diabetes.

We have adapted a polygenic mouse model of type II diabetes, the TALLYHO,<sup>14,15</sup> for modeling of CLTI using creation of an ischemic hindlimb to determine the ability of human

vBA-MSC to promote tissue perfusion and skeletal muscle regeneration and function. The goal of this study was to ascertain whether vBA-MSC administration could stimulate limb perfusion, improve muscle function, and facilitate muscle regeneration as assessed by multiple histological and molecular markers.

## METHODS

### Animals and CLTI Model

All studies followed the Public Health Service (PHS) Policy on Humane Care and Use of Laboratory Animals, were compliant with animal welfare guidelines as reviewed by the American Association for Laboratory Animal Science (AAALAC), and were approved by the Indiana University School of Medicine Institutional Animal Care and Use Committee. Specific pathogen-free TALLYHO/JngJ mice (male; Jackson Laboratory, Bar Harbor, ME) were received at 14 weeks of age and acclimated for a minimum of 1 week prior to use. Only TALLYHO male mice were used, because females do not express the diabetic phenotype.<sup>14</sup> TALLYHO male mice develop hyperglycemia, hyperinsulinemia, hyperlipidemia, moderate obesity, and enlargement of the islets of Langerhans.<sup>14,15</sup> These metabolic effects are more progressive in onset and reflect the genetic status of a large percentage of the human diabetic population compared to a monogenic model homozygous for a mutation, such as the *Lepr<sup>db</sup>* (db/db), which is carried by very few diabetes patients. Endothelial dysfunction also has been observed in the TALLYHO,<sup>16</sup> which is a prime characteristic of diabetes. Mice were identified by ear punch prior to surgery and housed at a maximum density of 5 per cage on sterilized contact bedding. Teklad 2018SX Global 18% Protein Extruded Rodent Diet (Inotiv, West Lafayette, IN) and acidified water were supplied ad libitum, and mice were housed in rooms with a 12-hour light or dark cycle at  $21 \pm 3^\circ\text{C}$ , with 30–80% relative humidity and at least 10 changes per hour of conditioned fresh air. Following acclimation, a severe ischemic model of CLTI was created via unilateral double ligation of the femoral artery above and below the inguinal ligament and ligation of collateral circulation, as previously described.<sup>17</sup>

Mice were randomly assigned to one of 4 cohorts, each consisting of 5 animals: cell-treated for sacrifice at 7 days, Veh treatment for sacrifice at 7 days, cell-treated for sacrifice at 30 days, and vehicle treatment for sacrifice at 30 days. No animals were sacrificed or lost due to necrosis-related mortality.

### Serum Glucose

Glucose in serum samples from nonfasting mice taken at the experiment endpoint was initially quantitated by analysis at the Translational Core of the Indiana University Center for Diabetes and Metabolic Diseases. Subsequent measurements were made with a True Metrix Pro glucometer (Trivida Health Inc., Fort Lauderdale, FL) at the time of surgery, day -8, and again at the time of tissue harvest on day 30. The results were comparable between the 2 methods. Mice were considered diabetic if nonfasting blood glucose was  $\geq 300$  mg/dL.<sup>18,19</sup>

## Laser Doppler Perfusion Imaging and Muscle Testing

Baseline limb perfusion and plantar flexion muscle testing (MT) prior to surgery was determined by laser Doppler perfusion imaging (LDPI) using a Moor LD12-HIR (Moor Instruments Inc., Wilmington, Delaware) and an Aurora Scientific 1310A in situ MT apparatus (Aurora, Ontario Canada), respectively. Measurements were conducted as per manufacturer guidelines, and LDPI and MT were performed longitudinally following model creation at the set intervals shown in Figure 1. Perfusion ratio was calculated using the contralateral, unligated limb as the control.

## Cell Preparation and Administration

vBA-MSC were obtained from Ossium Health, Indianapolis, Indiana, and cultured to a maximum of passage 6, as previously described.<sup>13</sup> The vBA-MSC express typical MSC surface markers (CD73, CD90, and CD105), expressed very low levels of hematopoietic cell surface markers as well as human leukocyte antigen class II proteins, and possess the potential to clonally expand and undergo trilineage differentiation.<sup>13</sup> Approximately, 7 days following CLTI model creation, a cohort of 5 mice were injected with 500,000 vBA-MSC into the gracilis muscle by 3 injections of approximately 50 microliters, not to exceed a total of 150 microliters (Fig. 1). A second cohort of 5 control mice was injected with an equal volume of Veh into the ischemic control limb gracilis muscle.

## Tissue Preparation and Histological Staining

At the appropriate time point, mice were anesthetized via isoflurane inhalation, and blood was collected via a closed chest stick from the left ventricle for serum glucose determination and for the preparation of serum. The thoracic cavity was opened, and the vasculature was perfused with ~3 ml phosphate buffered saline (PBS), including vascular dilator (0.1 mM adenosine and 0.01 mM sodium nitroprusside) via the left ventricle at 100–120 mm Hg. Following perfusion, muscles were dissected, cut in half, and either immersion-fixed in 10% neutral buffered formalin (NBF) or preserved in RNA *later* (Invitrogen or Thermo Fisher Scientific, Waltham, MA), and stored at –20°C until total RNA isolation. Formalin-fixed tissues were paraffin-embedded, sectioned, and then stained with hematoxylin and eosin (H and E) or picosirius red (PSR). Additional slides with unstained tissue sections were stored for immunohistochemistry.

To assess muscle fibrosis, relative collagen content in muscle was determined by using the thresholding function of ImageJ to measure the area of PSR staining, as previously described.<sup>20</sup> A threshold value of 90 was used to standardize values for PSR-stained areas between the samples.

To determine capillary density, formalin fixed paraffin embedded muscle sections were incubated with Trilogy pretreatment solution (Cell Marque Tissue Diagnostics, Rocklin, CA) for deparaffinization and antigen retrieval, washed with tris buffered saline with Tween-20, and blocked with 1x animal-free blocker (Vector Laboratories, Newark, CA). Sections were incubated with a 1:50 dilution of the endothelial-specific Griffonia Simplicifolia Lectin I isolectin-B4 (Vector) for 60 min, followed by washing and a second incubation with a 1:500 dilution of wheat germ agglutinin-555 lectin (Fisher or Invitrogen)

to label muscle fibers. Nuclei were detected by a 5-minute incubation period with a 1:500 dilution of 4',6-diamidino-2-phenylindole, and tissues were cover-slipped with Vector Express (Vector). Fluorescent images were obtained for 3–5 representative sections from 2–3 nonsequential serial sections per mouse muscle, and capillaries were counted in a field of view and normalized to fiber number.

Digital images of muscle sections were acquired with a Leica DM 5000B microscope, a DMC 6200 digital camera, and Leica Application Suite X imaging software (Leica Microsystems, Inc., Buffalo Grove, IL, USA). Multiple nonsequential serial tissue sections (2–3) from each mouse muscle were evaluated for histopathological characteristics. Morphometric measurements were made from stored images with Image J.

### Real-Time Quantitative polymerase chain reaction (PCR)

Relative differences in muscle mRNA expression for various molecules were determined using reverse transcription real-time quantitative PCR (RT-qPCR), as previously described in detail.<sup>21</sup> For PCR, aliquots of copy DNA (5.0  $\mu$ l, 1: 25 dilution) were combined with primers and probes (TaqMan Gene Expression Assays; Thermo Fisher or Applied Biosystems) for the genes MyH3 (embryonic myosin heavy chain), MyoD1 (Myogenic differentiation 1), Mrc1 (mannose receptor C-Type 1; CD206), VEGF-A (vascular endothelial growth factor A), NCF1 (p47phox; neutrophil cytosolic factor 1), IL-10 (interleukin 10), FoxP3 (Forkhead box protein P3), or hypoxanthine-guanine phosphoribosyl-transferase (HPRT) as the endogenous control in the presence of a PCR master mix (TaqMan Fast Advanced Master Mix; Thermo Fisher or Applied Biosystems). Triplicate reactions were run on an Applied Biosystems 7,500 real-time PCR system using relative quantification double delta threshold cycle with standard two-step 7500 PCR cycling conditions (40–45 cycles). Differences in PCR product yields between groups were determined by comparing the fold differences between target mRNA after normalization to HPRT.

## RESULTS

### Serum Glucose

Serum glucose concentration was measured in nonfasting mice and was not significantly different between Veh and cell-treated groups, confirming a diabetic phenotype and demonstrating that vBA-MSC administration had no effect on glucose (Fig. 2). Because the diabetic phenotype is not fully penetrant in the male TALLYHO mice, blood glucose measurements were made at the time of CLTI model creation as well as at tissue harvest. The prevalence of the nondiabetic phenotype ( $< 300$  mg/dl) was approximately 10% of the total mice number.

### Hindlimb Muscle Perfusion and Function

Hindlimb muscle perfusion was determined via LDPI prior to surgery to determine a baseline, 1 day following surgery to assess the decrease in perfusion and then at approximately 7-day intervals up to the time of euthanasia (Fig. 3). Injection of vBA-MSC was performed 7 days after model creation to allow the establishment of preexisting ischemic damage and to allow time for reduction in surgery-induced inflammation. This

method is a better approximation of the clinical situation for cell therapy as opposed to the common practice of administering cells at the time of model creation. Perfusion was initially stimulated above Veh controls at 10 days following vBA-MSC injection, but then decreased below control values (Fig. 3), a result consistent with the use of human cells in an immunocompetent mouse model. Muscle function also was determined longitudinally by measuring plantar flexion torque at multiple stimulation frequencies. While no difference was detected in peak torque (not shown), vBA-MSC-treated mice had significantly reduced muscle fatigue in the ischemic hindlimb compared to Veh-treated ischemic control limbs (Fig. 4).

### **vBA-MSC and Muscle Pathology**

Gastrocnemius muscle sections were evaluated 30 days following cell injection for characteristics of ischemic damage, including the presence of polymorphic fibers, necrotic fibers, small regenerating fibers, regenerated fibers, intramuscular adipocytes, intramuscular macrophages, and collagen deposition. Nonischemic control tissue showed normal histology, whereas ischemic muscle exhibited monomorphic myocytes with centralized nuclei, macrophages and cellular infiltrates, necrotic fibers, and significant presence of adipocytes (Fig. 5). Paraffin-embedded sections of muscle from vBA-MSC-treated mice were observed to have isolated areas of fibers with centralized nuclei, suggesting regeneration and significantly reduced infiltrates and adipocytes compared to ischemic gastrocnemius muscle. Similar results were seen with control, ischemic, and vBA-MSC-treated tibialis muscle (results not shown).

The PSR-stained gastrocnemius muscle was analyzed to determine potential changes in collagen content and expressed as a percentage of total tissue area. Collagen was increased in ischemic Veh-treated hindlimb muscle 30 days post-CLTI model creation but was reduced to near nonischemic control levels in vBA-MSC-treated mice (Fig. 6).

### **vBA-MSC-Stimulated Angiogenesis**

To determine the ability of vBA-MSC administration to stimulate angiogenesis in ischemic muscle, capillary density in lectin-stained gastrocnemius and tibialis muscle sections was determined. The results indicated that a significant increase in capillary density was present 30 days after injection of vBA-MSC compared to Veh controls in tibialis, but not the gastrocnemius muscle (Fig. 7).

### **Expression Changes for Muscle Regeneration and Angiogenesis-Related Molecular Markers**

Molecular markers associated with muscle regeneration include embryonic myosin heavy chain (MyH3) and myoblast determination protein 1 (MyoD1).

The assessment of mRNA expression using real-time PCR showed that both markers were significantly increased in the gastrocnemius muscle treated with vBA-MSC compared to Veh-treated control muscle 7 days following cell injection (Fig. 8A, B).

Molecular markers related to T regulatory cell presence and function were also examined, which included forkhead Box P3 protein (FoxP3) and IL-10. Both markers were elevated in vBA-MS-C-treated gastrocnemius muscle compared to Veh-treated controls 30 and 7 days after cell injection, respectively. (Fig. 9A, B).

Muscle regeneration is known to be highly dependent on the presence of the M2-biased macrophage phenotype,<sup>22</sup> thus mRNA expression of the mannose receptor C-Type 1 (Mrc1/CD206) was determined. The injection of vBA-MS-C significantly increased Mrc1 mRNA expression at 7 days after injection compared to Veh alone as determined by PCR analysis (Fig. 10).

Because an increase in capillary density or angiogenesis had been observed (Fig. 7) following administration of vBA-MS-C, expression of VEGF-A, a known angiogenic growth factor, was measured. VEGF-A mRNA expression was slightly increased in gastrocnemius and tibialis 7 days following cell injection, and its expression remained increased through 30 days, consistent with greater capillary density observed at 30 days (Fig. 11).

## DISCUSSION

The current study was undertaken with the goal of determining the extent to which vBA-MS-C could ameliorate muscle damage from hindlimb ischemia similar to that associated with human diabetic CLTI. A polygenic diabetic mouse model, the TALLYHO, was adopted to more accurately model human noninsulin-dependent type 2 diabetes mellitus. TALLYHO male mice develop hyperglycemia, hyperinsulinemia, hyperlipidemia, moderate obesity, and enlargement of the islets of Langerhans<sup>14,15</sup> as well as endothelial dysfunction,<sup>16</sup> a prime characteristic of diabetes. While numerous studies have been performed using a variety of stem cells or MSC with a rodent ischemic hindlimb model,<sup>23–27</sup> only one study to date, that we are aware of, was done in the context of genetic diabetes.<sup>28</sup> However, it was performed using monogenic leptin knock out mice, which are representative of only a small percentage of diabetic patients. To the authors' knowledge there are no other publications demonstrating successful treatment of an immunocompetent polygenic diabetic murine model of hindlimb ischemia using cell therapy.

A distinct feature of the current study is the use of an immunocompetent mouse. A large number of human cell therapy studies have been conducted using immunocompromised mouse strains, such as Nod-severe combined immunodeficient or BALBc.<sup>24,27,29,30</sup> While an immunocompromised state allows for extended survival time of foreign cells, the use of immunocompetent mice more appropriately mirrors the therapeutic effect experienced in humans. Accordingly, there is a limitation to cell viability in immunocompetent subjects, and allogeneic cells remain viable for only a few days. This short viability period is consistent with the observed transient effects of vBA-MS-C on limb perfusion (Fig. 3), although other factors may be involved. Arpino et al.<sup>31</sup> have demonstrated that the presence of angiogenesis does not correspond to functional recovery of flow following ischemic injury, and this finding corresponds to the observation that VEGF-A expression was increased at 30 days (Fig. 11) despite a decrease in limb perfusion. However, other paracrine effects of MSC may be longer lasting in the same setting. Results from our

laboratory investigating the effect of human MSC administration on IL-10 levels in an immunocompetent C57BL/6 model demonstrated a transient rise in human IL-10 levels followed by an increase in mouse IL-10 for the subsequent 21 days.<sup>32</sup> This result suggests that despite a relatively brief lifespan in immunocompetent subjects, MSCs are able to exhibit a potent paracrine effect that influences native cell activity.

Another departure in the current study from a majority of hindlimb ischemia studies is the timing of treatment. Most studies to date using cell therapy to treat CLTI modeled via femoral artery ligation use one timepoint for both model creation (ligation) and treatment (cell injection) leaving no ischemic window. The current model instead induces ischemia with treatment occurring 7 days after vessel ligation. The rationale for this delay is to evade the inflammatory cascade that is activated as a response to ischemic insult. Thus, this design avoids any confounding increase in circulating cytokines due to an innate ischemic response by waiting until after its resolution and ensures that molecular changes are due to cell treatment alone.

In the setting of inflammation and ischemic muscle damage, muscle regeneration is dependent on a distinct behavior of macrophages, known as phenotypic switching, in which macrophages transition between the M1-biased (pro-inflammatory) phenotype and the M2-biased (anti-inflammatory) phenotype.<sup>33</sup> The M2 phenotype is known to be involved in muscle regeneration through regulation of T regulatory cells.<sup>22</sup> Our data is consistent with this principle, as the overall results demonstrated that exogenous vBA-MSC treatment promoted muscle regeneration via an IL-10 or FoxP3-mediated M1-M2 phenotypic shift. In addition to T regulatory-mediated pathways, muscle regeneration stimulated by vBA-MSC was further confirmed by upregulation of independent markers of muscle regeneration, MyH3, and MyoD1, with an associated angiogenic response demonstrated by increased expression of VEGF-A.

## Limitations

While some aspects of the current study are novel, several limitations must be noted. Inherent limitations exist with the TALLYHO mouse, such as the diabetic phenotype being limited to males and the lack of a suitable genetic control factors that may limit translatability to human subjects. The Swiss mouse has been suggested as a control for the TALLYHO and it also has been used as a model for hindlimb ischemia,<sup>34</sup> thus, it was examined as a potential alternative control using the CLTI severe ischemia model; however, results showed that it was extremely sensitive to severe limb ischemia, resulting in early euthanasia due to limb loss, making it unsuitable. The TALLYHO also displays progressive baseline perfusion recovery following creation of the CLTI model, which was unexpected in a diabetic mouse. The variability observed in the mRNA expression of certain molecular markers may have been due to natural animal variability or variability due to mechanical constraints in the consistent delivery of vBA-MSC into the muscle. There additionally exists the possibility that the paracrine effects of exogenous human MSC may not parallel murine cells due to differences in the cytokine structure and receptor function between species; thus, the effects of human MSC may be muted compared to potential effect of murine MSC.

Finally, to the authors knowledge, there are no atherosclerotic CLTI murine models to mirror that of what is experienced in human CLTI secondary to atherosclerotic disease progression.

Future work by our group will include alginate hydrogel encapsulation of MSCs to amplify the paracrine effects of the cells by protecting them from immune-mediated destruction. Additional studies to alter the phenotype of MSCs to produce more anti-inflammatory and regenerative cytokines are also planned, including pretreatment at low oxygen tension and/or high glucose concentrations to mimic microenvironmental conditions in ischemic diabetic muscle<sup>35-37</sup> as well as genetic modification to produce vBA-MSC overexpressing IL-10 and/or IL-33, which are known to participate in muscle regeneration.<sup>38,39</sup> Additional experiments to investigate the impact of cell therapy on fibro or adipogenic progenitors (FAP) and muscle satellite cells also will be conducted.

## CONCLUSIONS

The current study was undertaken with a polygenic diabetic mouse model to better model human type 2 diabetes and with the goal of assessing the ability of vBA-MSC to ameliorate damage from muscle ischemia. Taken together, the results indicate that vBA-MSCs can reverse ischemic muscle damage, reduce inflammation, and increase muscle function by promoting transient increases in perfusion, regeneration of muscle fibers, and angiogenesis. The abundance, ready availability, and characteristics of bone-adherent MSC derived from vertebral bodies thus make them a more practical cell type for use in CLTI patients and warrant further investigation to develop strategies for human use.

## Funding:

This work was supported by the Cryptic Masons Medical Research Foundation, Brownsburg, IN. Other than financial support, the Foundation had no role in the creation or submission of this article.

We thank Patrick Mason for assisting with real-time PCR.

## REFERENCES

1. Creager MA, Matsushita K, Arya S, et al. Reducing nontraumatic lower-extremity amputations by 20% by 2030: time to get to our feet: a policy statement from the American heart association. *Circulation* 2021;143:e875–91. [PubMed: 33761757]
2. Smith AD, Hawkins AT, Schaumeier MJ, et al. Predictors of major amputation despite patent bypass grafts. *J Vasc Surg* 2016;63:1279–88. [PubMed: 26860641]
3. Farber A Chronic limb-threatening ischemia. *N Engl J Med* 2018;379:171–80. [PubMed: 29996085]
4. Rudofker EW, Hogan SE, Armstrong EJ. Preventing major amputations in patients with critical limb ischemia. *Curr Cardiol Rep* 2018;20:74. [PubMed: 29992515]
5. Durdu S, Akar AR, Arat M, et al. Autologous bone-marrow mononuclear cell implantation for patients with Rutherford grade II-III thromboangiitis obliterans. *J Vasc Surg* 2006;44: 732–9. [PubMed: 16926085]
6. Miyamoto K, Nishigami K, Nagaya N, et al. Unblinded pilot study of autologous transplantation of bone marrow mononuclear cells in patients with thromboangiitis obliterans. *Circulation* 2006;114:2679–84. [PubMed: 17145986]
7. Murphy MP, Lawson JH, Rapp BM, et al. Autologous bone marrow mononuclear cell therapy is safe and promotes amputation-free survival in patients with critical limb ischemia. *J Vasc Surg* 2011;53:1565–1574.e1. [PubMed: 21514773]

8. Powell RJ, Marston WA, Berceli SA, et al. Cellular therapy with Ixmyelocel-T to treat critical limb ischemia: the randomized, double-blind, placebo-controlled RESTORE-CLI trial. *Mol Ther* 2012;20:1280–6. [PubMed: 22453769]
9. Wang SK, Green LA, Gutwein AR, et al. Ethnic minorities with critical limb ischemia derive equal amputation risk reduction from autologous cell therapy compared with whites. *J Vasc Surg* 2018;68:560–6. [PubMed: 29503004]
10. Spreen MI, Gremmels H, Teraa M, et al. Diabetes is associated with decreased limb survival in patients with critical limb ischemia: pooled data from two randomized controlled trials. *Diabetes Care* 2016;39:2058–64. [PubMed: 27612499]
11. Teraa M, Gremmels H, Wijnand JGJ, et al. Cell therapy for chronic limb-threatening ischemia: current evidence and future directions. *Stem Cells Transl Med* 2018;7: 842–6. [PubMed: 30070050]
12. Chinnadurai R, Rajan D, Ng S, et al. Immune dysfunctionality of replicative senescent mesenchymal stromal cells is corrected by IFN $\gamma$  priming. *Blood Adv* 2017;1: 628–43. [PubMed: 28713871]
13. Johnstone BH, Miller HM, Beck MR, et al. Identification and characterization of a large source of primary mesenchymal stem cells tightly adhered to bone surfaces of human vertebral body marrow cavities. *Cytotherapy* 2020;22:617–28. [PubMed: 32873509]
14. Leiter EH, Strobel M, O'Neill A, et al. Comparison of two new mouse models of polygenic type 2 diabetes at the Jackson laboratory, NONcNZO10Lt/J and TALLYHO/JngJ. *J Diabetes Res* 2013;2013:165327. [PubMed: 23671854]
15. Tamarai K, Bhatti JS, Reddy PH. Molecular and cellular bases of diabetes: focus on type 2 diabetes mouse model-TallyHo. *Biochim Biophys Acta Mol Basis Dis* 2019;1865: 2276–84. [PubMed: 31082469]
16. Kim JH, Saxton AM. The TALLYHO mouse as a model of human type 2 diabetes. *Methods Mol Biol* 2012;933:75–87. [PubMed: 22893402]
17. Distasi MR, Case J, Ziegler MA, et al. Suppressed hindlimb perfusion in Rac2 $^{-/-}$  and Nox2 $^{-/-}$  mice does not result from impaired collateral growth. *Am J Physiol Heart Circ Physiol* 2009;296:H877–86. [PubMed: 19151256]
18. King AJ. The use of animal models in diabetes research. *Br J Pharmacol* 2012;166:877–94. [PubMed: 22352879]
19. Leiter EH. Selecting the “right” mouse model for metabolic syndrome and type 2 diabetes research. *Methods Mol Biol* 2009;560:1–17. [PubMed: 19504239]
20. Schipke J, Brandenberger C, Rajces A, et al. Assessment of cardiac fibrosis: a morphometric method comparison for collagen quantification. *J Appl Physiol (1985)* 2017;122:1019–30. [PubMed: 28126909]
21. Miller SJ, Coppinger BJ, Zhou X, et al. Antioxidants reverse age-related collateral growth impairment. *J Vasc Res* 2010;47:108–14. [PubMed: 19729957]
22. Schiaffino S, Pereira MG, Ciciliot S, et al. Regulatory T cells and skeletal muscle regeneration. *FEBS J* 2017;284: 517–24. [PubMed: 27479876]
23. Bhang SH, Cho SW, La WG, et al. Angiogenesis in ischemic tissue produced by spheroid grafting of human adipose-derived stromal cells. *Biomaterials* 2011;32:2734–47. [PubMed: 21262528]
24. Kang WC, Oh PC, Lee K, et al. Increasing injection frequency enhances the survival of injected bone marrow derived mesenchymal stem cells in a critical limb ischemia animal model. *Korean J Physiol Pharmacol* 2016;20: 657–67. [PubMed: 27847443]
25. Koch JM, D'Souza SS, Schwahn DJ, et al. Mesenchymoangioblast-derived mesenchymal stromal cells inhibit cell damage, tissue damage and improve peripheral blood flow following hindlimb ischemic injury in mice. *Cytotherapy* 2016;18:219–28. [PubMed: 26740280]
26. Lian Q, Zhang Y, Zhang J, et al. Functional mesenchymal stem cells derived from human induced pluripotent stem cells attenuate limb ischemia in mice. *Circulation* 2010;121:1113–23. [PubMed: 20176987]
27. Prather WR, Toren A, Meiron M, et al. The role of placental-derived adherent stromal cell (PLX-PAD) in the treatment of critical limb ischemia. *Cytotherapy* 2009;11: 427–34. [PubMed: 19526389]

28. Liew A, Baustian C, Thomas D, et al. Allogeneic mesenchymal stromal cells (MSCs) are of comparable efficacy to syngeneic MSCs for therapeutic revascularization in C57BKSDb/db mice despite the induction of alloantibody. *Cell Transplant* 2018;27:1210–21. [PubMed: 30016879]
29. Lee JH, Han YS, Lee SH. Long-duration three-dimensional spheroid culture promotes angiogenic activities of adipose-derived mesenchymal stem cells. *Biomol Ther (Seoul)* 2016;24:260–7. [PubMed: 26869524]
30. Park IS, Chung PS, Ahn JC. Enhanced angiogenic effect of adipose-derived stromal cell spheroid with low-level light therapy in hind limb ischemia mice. *Biomaterials* 2014;35: 9280–9. [PubMed: 25132605]
31. Arpino JM, Nong Z, Li F, et al. Four-dimensional microvascular analysis reveals that regenerative angiogenesis in ischemic muscle produces a flawed microcirculation. *Circ Res* 2017;120:1453–65. [PubMed: 28174322]
32. Wang SK, Green LA, Gutwein AR, et al. Rationale and design of the ARREST trial investigating mesenchymal stem cells in the treatment of small abdominal aortic aneurysm. *Ann Vasc Surg* 2018;47:230–7. [PubMed: 28916304]
33. De Santa F, Vitiello L, Torcinaro A, et al. The role of metabolic remodeling in macrophage polarization and its effect on skeletal muscle regeneration. *Antioxid Redox Signal* 2019;30:1553–98. [PubMed: 30070144]
34. Lejay A, Choquet P, Thaveau F, et al. A new murine model of sustainable and durable chronic critical limb ischemia fairly mimicking human pathology. *Eur J Vasc Endovasc Surg* 2015;49:205–12. [PubMed: 25579876]
35. He Y, Chen JF, Yang YM, et al. CKIP-1 regulates the immunomodulatory function of mesenchymal stem cells. *Mol Biol Rep* 2019;46:3991–9. [PubMed: 31168669]
36. Liu J, Hao H, Xia L, et al. Hypoxia pretreatment of bone marrow mesenchymal stem cells facilitates angiogenesis by improving the function of endothelial cells in diabetic rats with lower ischemia. *PLoS One* 2015;10:e0126715. [PubMed: 25996677]
37. Phelps J, Hart DA, Mitha AP, et al. Physiological oxygen conditions enhance the angiogenic properties of extracellular vesicles from human mesenchymal stem cells. *Stem Cell Res Ther* 2023;14:218. [PubMed: 37612731]
38. Bartolacci JG, Behun MN, Warunek JP, et al. Matrix-bound nanovesicle-associated IL-33 supports functional recovery after skeletal muscle injury by initiating a pro-regenerative macrophage phenotypic transition. *NPJ Regen Med* 2024;9:7. [PubMed: 38280914]
39. Kuswanto W, Burzyn D, Panduro M, et al. Poor repair of skeletal muscle in aging mice reflects a defect in local, interleukin-33-dependent accumulation of regulatory T cells. *Immunity* 2016;44:355–67. [PubMed: 26872699]

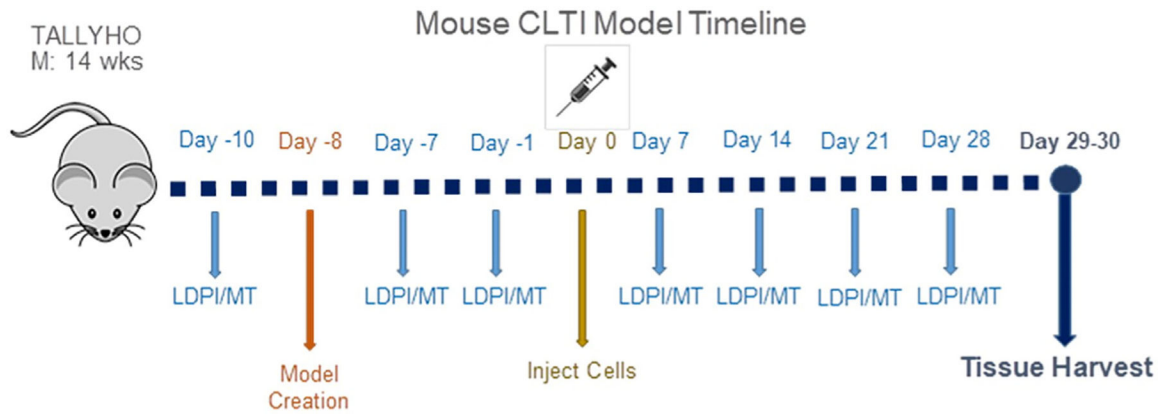


**Fig. 1.** Timeline of surgery, cell delivery, LDPI, plantar flexion MT, and endpoint for the TALLYHO CLTI model.

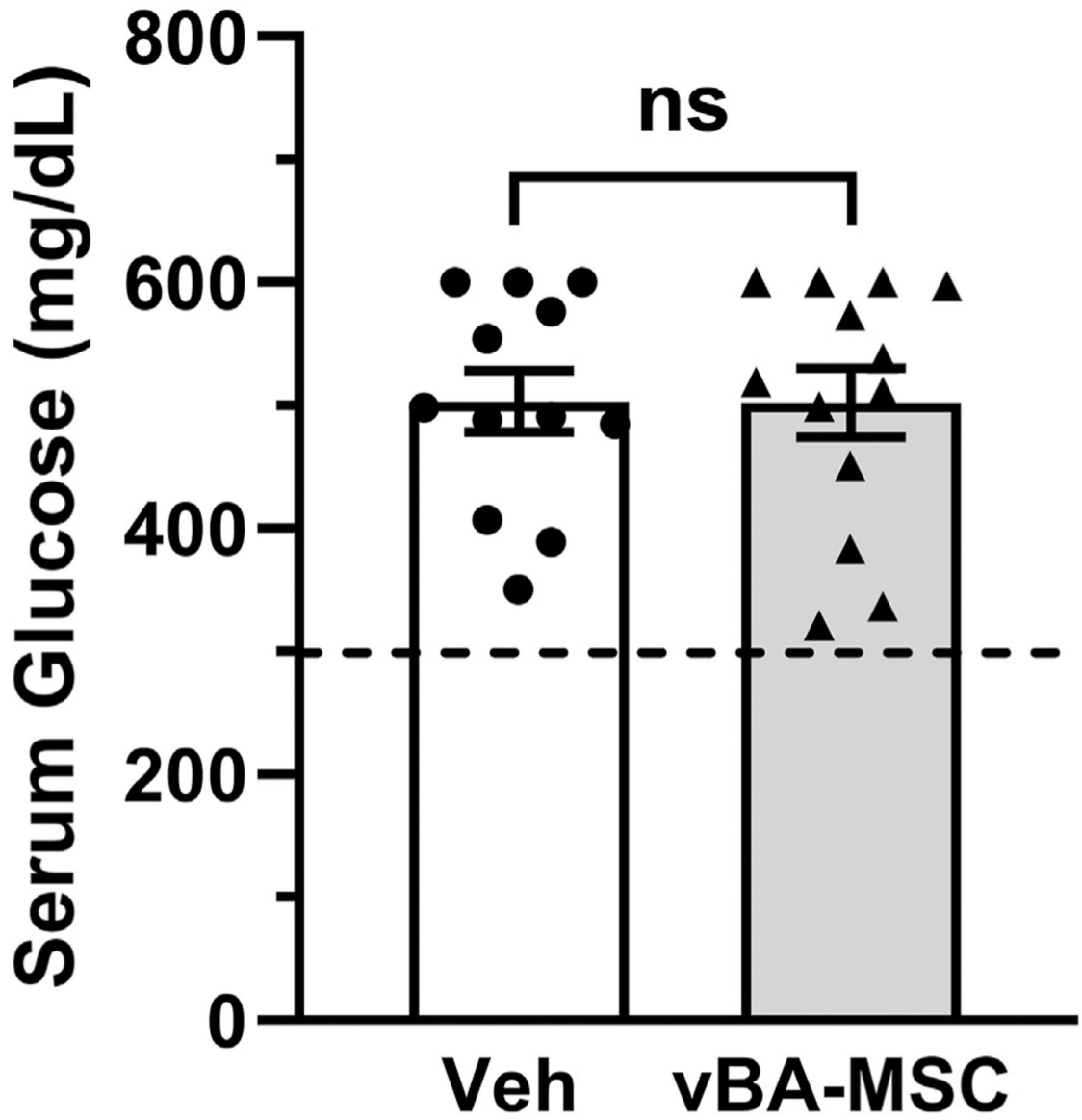


**Fig. 2.** Serum glucose is not impacted by vBA-MSC. The mean nonfasting serum glucose concentrations determined via a glucometer in the untreated (Veh) and vBA-MSC-treated (MSC) mice were  $503 \pm 25$  and  $502 \pm 28$  mg/dL, respectively. The dotted line indicates glucose concentration cutoff for diabetic mice.

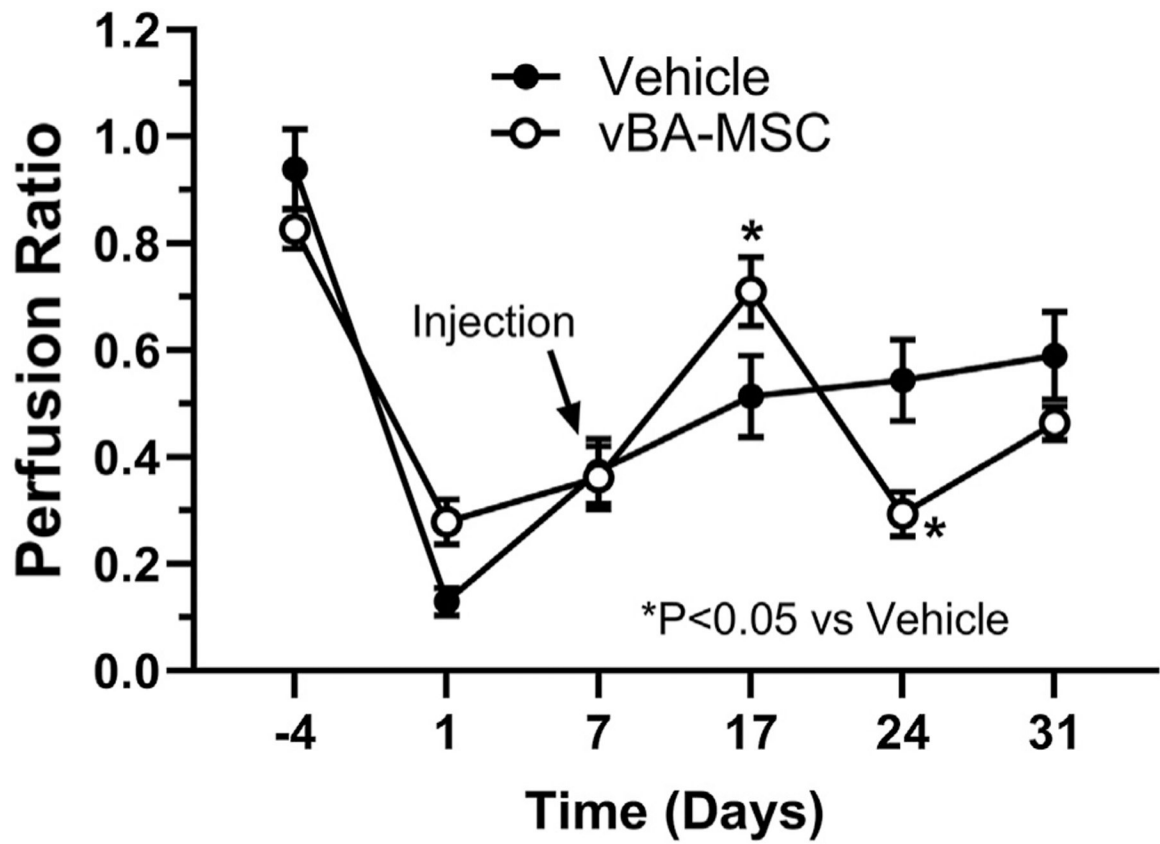


**Fig. 3.** Longitudinal measurement of TALLYHO hindlimb blood perfusion ratio (ligated or control). The perfusion ratio significantly increased in vBA-MSC-treated mice 10 days postinjection compared to Veh controls but fell below Veh values 2 weeks postinjection ( $n = 5/\text{group}$ ).

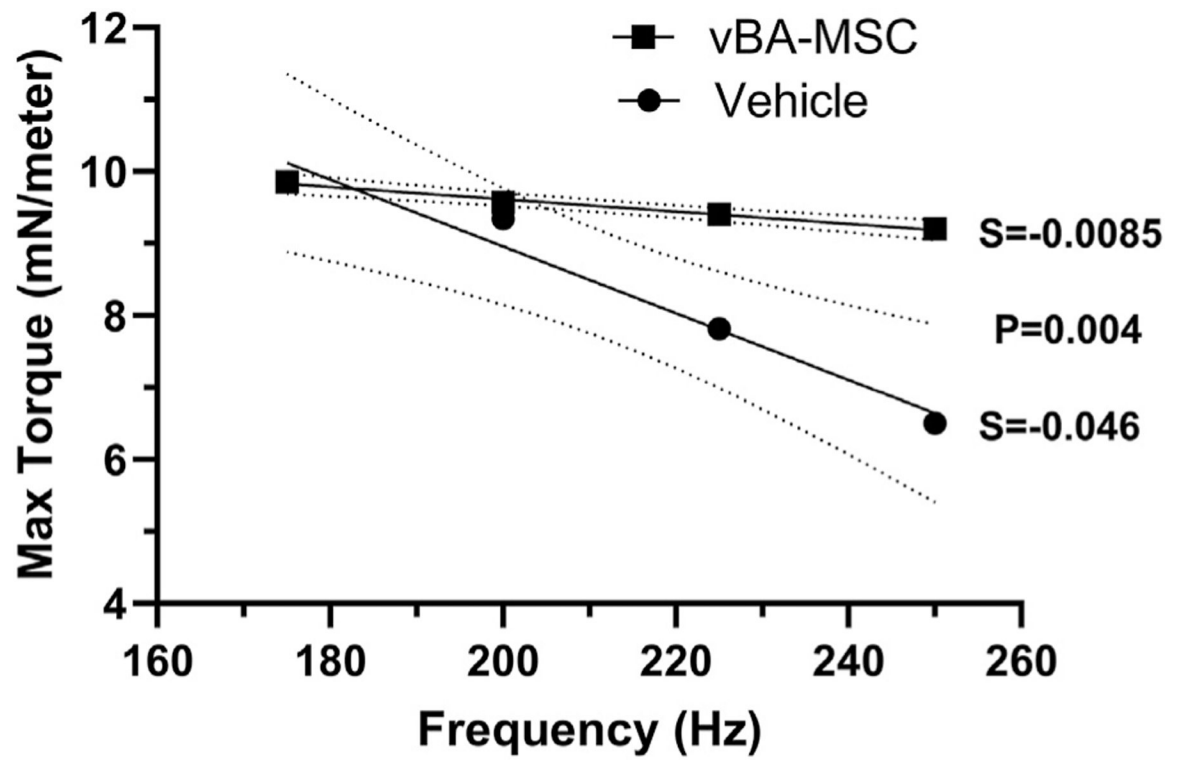


**Fig. 4.** vBA-MSC improved muscle function. Linear regression analysis of plantar flexion muscle torque over a range of stimulation frequencies showed that vBA-MSC-treated ischemic muscle had significantly less fatigue than Veh-treated ischemic muscle 28 days following cell injection ( $n = 5/\text{group}$ ).

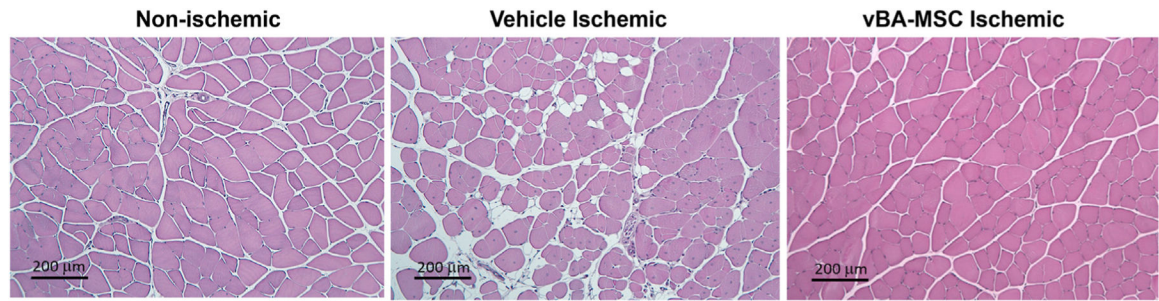


**Fig. 5.** vBA-MSC initiate muscle regeneration. Representative images of H and E-stained gastrocnemius muscle from non-ischemic control, Veh-treated ischemic, and vBA-MSC-treated ischemic gastrocnemius 30 days following cell injection.

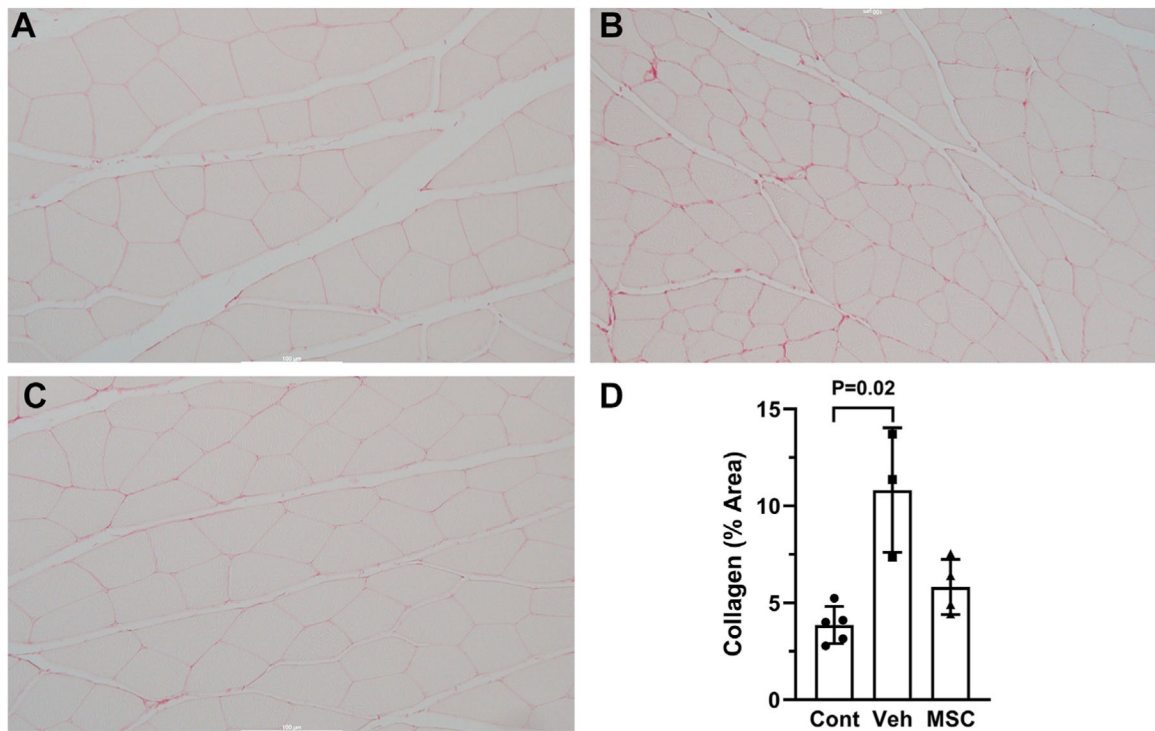


**Fig. 6.** vBA-MSC reduced fibrosis in ischemic muscle. Representative images of PSR-stained gastrocnemius muscle (mag = 200X) are shown from (A) nonischemic control, (B) ischemic Veh-treated, and (C) ischemic vBA-MSC-treated mice, respectively. (D) Collagen was quantified by threshold analysis with National Institutes of Health ImageJ, and the results indicated significantly increased collagen deposition in the ischemic gastrocnemius muscle (Veh) compared to the nonischemic control (Cont) muscle. vBA-MSC treatment (MSC) decreased ischemic muscle fibrosis to near control levels.

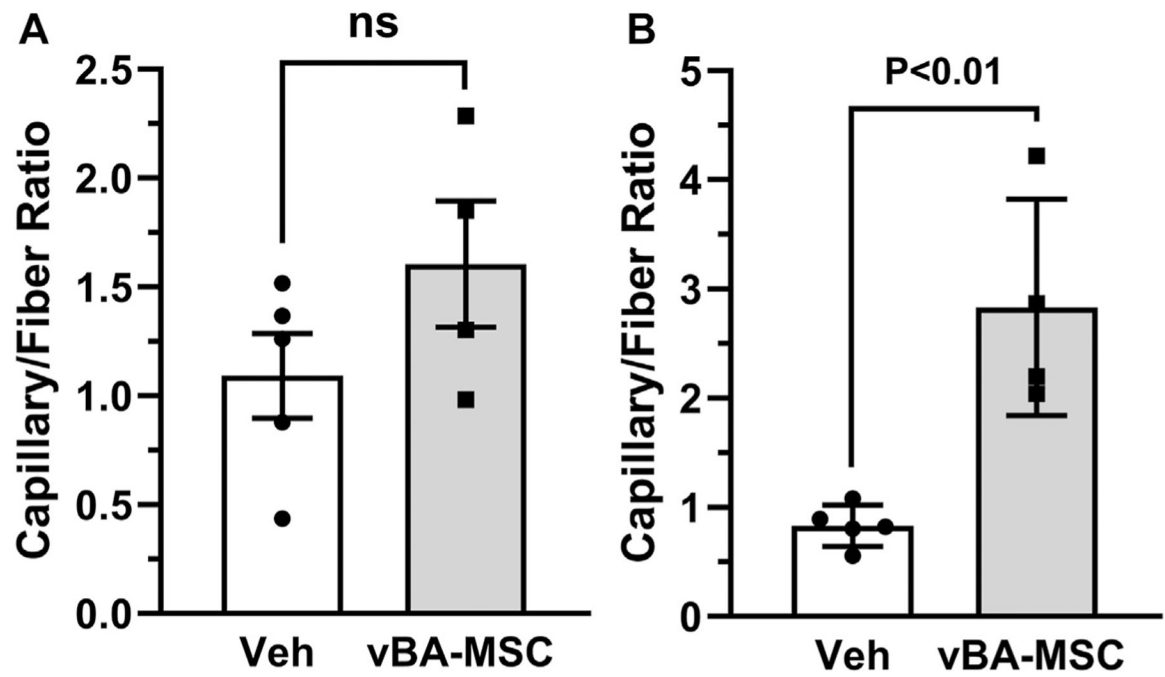


**Fig. 7.** Capillary density in ischemic hindlimb muscles. The capillary to fiber ratio was determined as an index of muscle angiogenesis in (A) gastrocnemius and (B) tibialis from Veh (Veh) and vBA-MSC-treated mice.

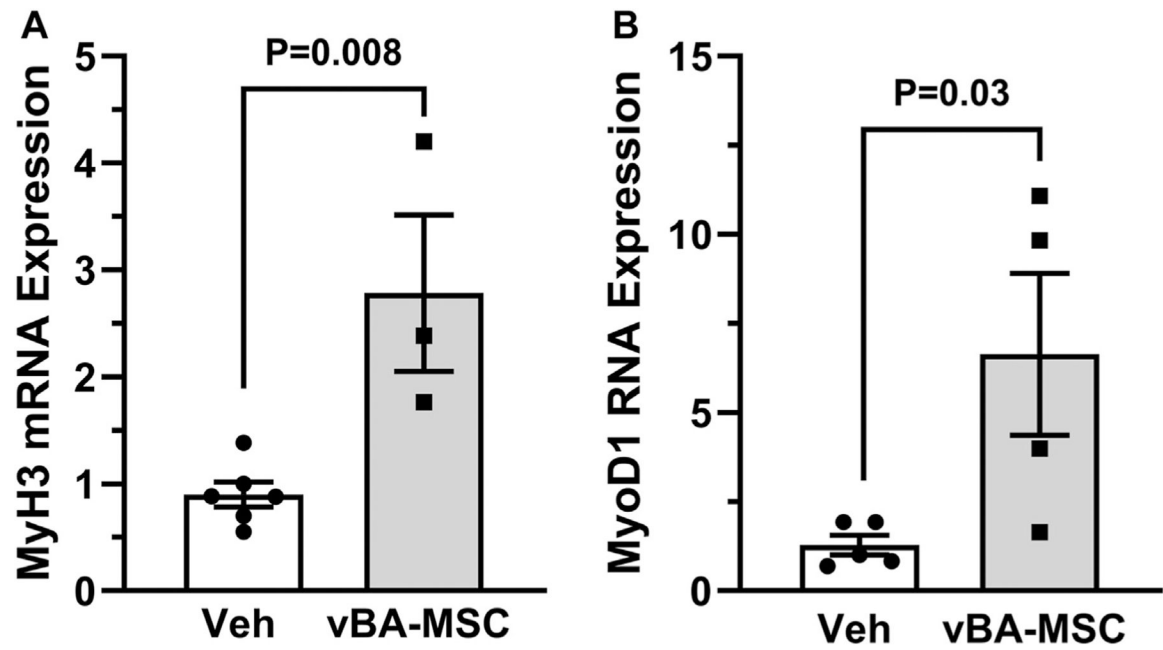


**Fig. 8.** PCR analysis of muscle regeneration markers. Relative expression changes for (A) embryonic myosin heavy chain (MyH3), and (B) myoblast determination protein 1 (MyoD1) mRNA in ischemic Veh and vBA-MSC-treated gastrocnemius muscle were determined by real-time PCR 7 days after cell injection.

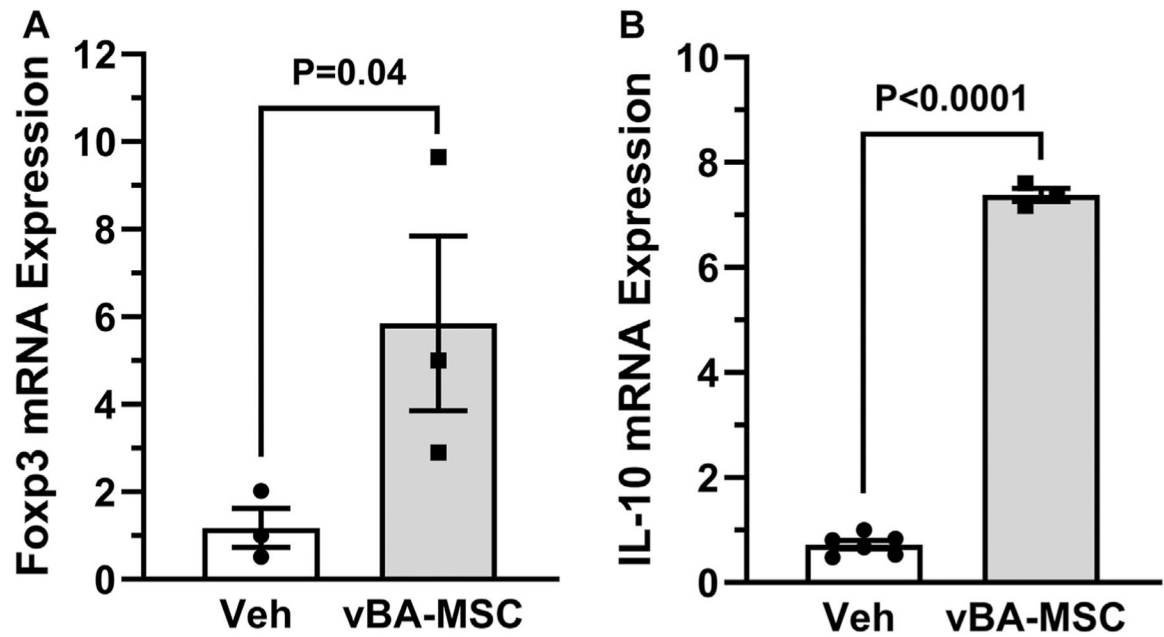


**Fig. 9.** PCR analysis of markers related to Treg function. **(A)** Relative expression change for murine forkhead Box P3 protein (FoxP3) versus Veh control (Veh) in the ischemic gastrocnemius muscle was determined 30 days following cell injection. **(B)** IL-10 expression was determined 7 days following cell injection.

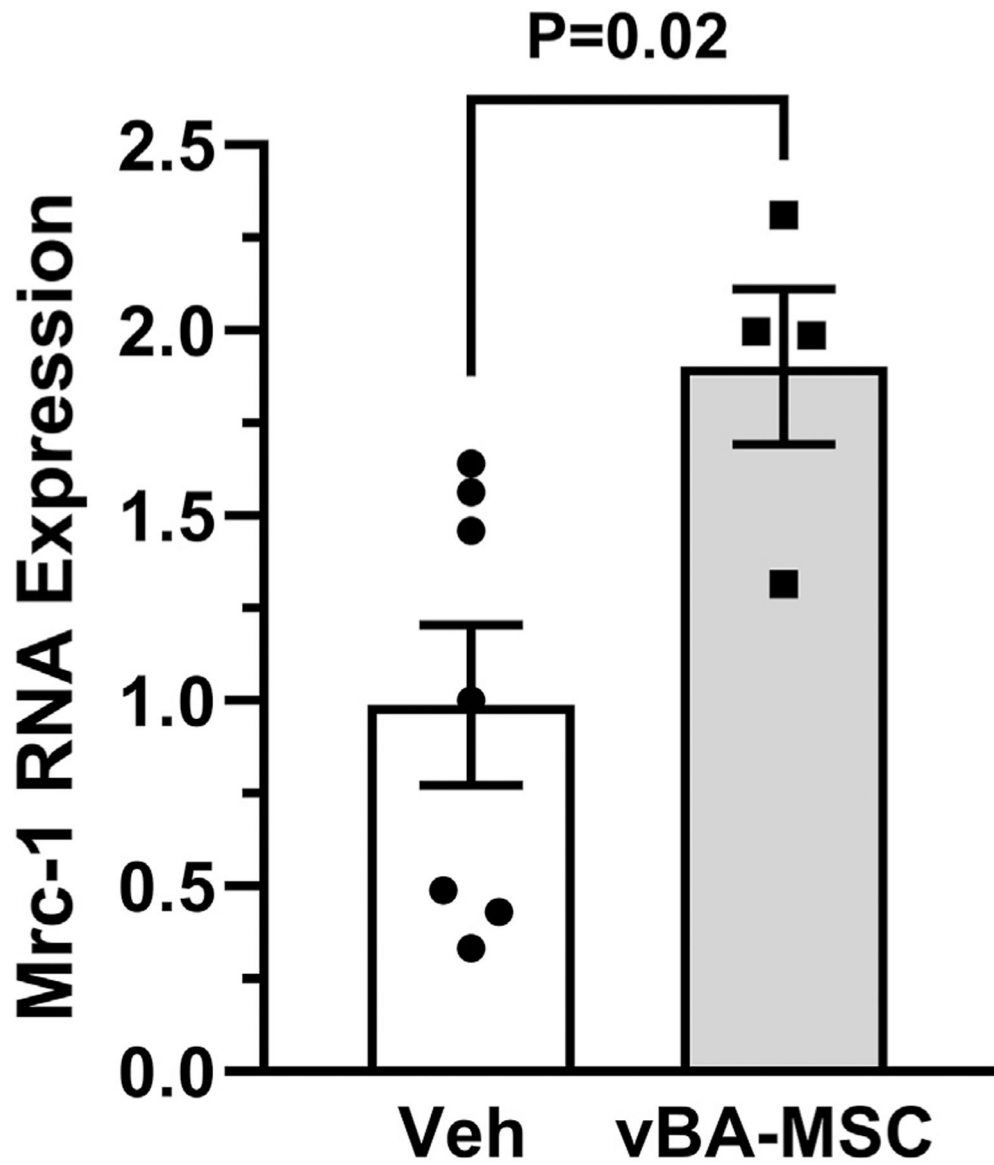


**Fig. 10.** vBA-MSc stimulate regenerative macrophages. M2-biased macrophage marker Mrc1 (CD206) mRNA expression was determined in Veh-treated and vBA-MSc-treated gastrocnemius muscle by real-time PCR at 7 days following cell injection.

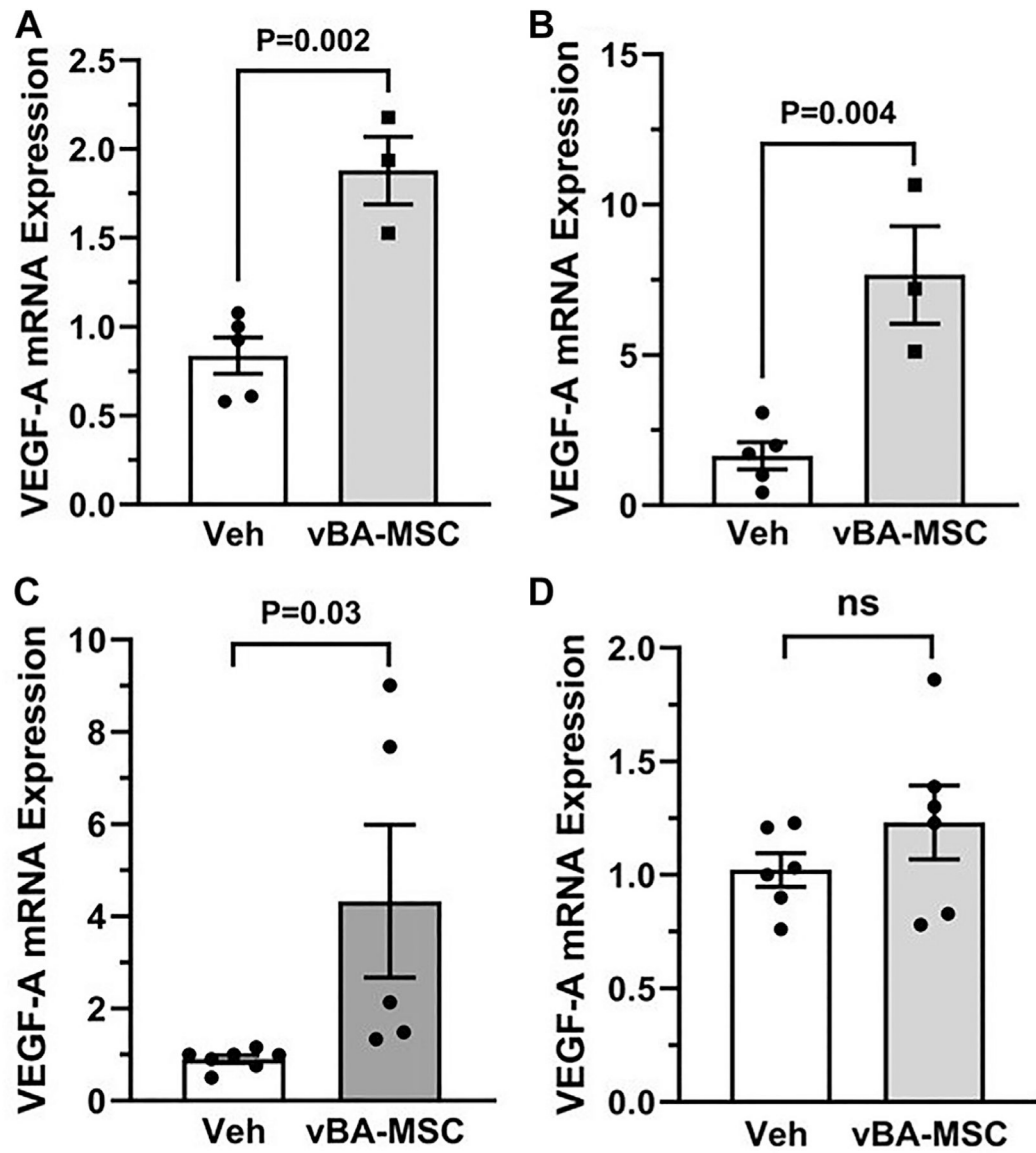


**Fig. 11.** vBA-MSc stimulate an angiogenic factor. VEGF-A mRNA expression was determined in Veh-treated and vBA-MSc-treated ischemic gastrocnemius by real-time PCR at (A) 7 days and (B) 30 days after cell injection as well as tibialis at (C) 7 days and (D) 30 days.